

H.E.S.S.: Astronomy above 10^{11} eV

Wystan Benbow

Max Planck Institut für Kernphysik, Postfach 103980, 69029 Heidelberg, Germany

The High Energy Stereoscopic System (H.E.S.S.), a third-generation array of atmospheric-Cherenkov telescopes, is used to perform searches for VHE (>100 GeV; Very High Energy) γ -ray emission from astrophysical objects with unprecedented sensitivity (5σ detection of a 1% Crab flux source in ~ 25 hours of observation). Prior to the commencement of H.E.S.S. observations, only ~ 10 sources of VHE γ -rays were known. With the recent detections by H.E.S.S. of more than 30 sources of VHE γ -rays, from a number of source classes, the understanding of the VHE sky has dramatically improved. Highlights of recent results are presented.

1. INTRODUCTION

Although the sky is opaque to VHE (>100 GeV) photons, astronomy above this energy requires a ground-based instrument, since satellite-borne detectors are too small to detect the low source fluxes at these energies. Imaging atmospheric-Cherenkov telescopes (IACTs) are commonly used to search for astrophysical γ -ray emission above ~ 100 GeV up to ~ 100 TeV. These instruments detect the flashes of Cherenkov light emitted from the electromagnetic cascade of secondary particles (EAS; Extensive Air Shower) resulting from the initial interaction of a γ -ray primary in the upper atmosphere. Astronomical observations are possible since an EAS and its Cherenkov light-pool retain the original direction of the incident photon to a high degree. An accurate determination of the primary photon's energy also can be made since the number of Cherenkov photons generated by an EAS is strongly correlated with this energy. Unfortunately, γ -ray observations are severely limited by charged cosmic-ray particles which are $\sim 10,000$ times more numerous than a photon of a given energy, and which produce superficially similar EAS. However, by imaging the Cherenkov light-pool, subtle differences between the cascades initiated by photons and hadronic particles can be exploited to reject almost all of the cosmic-ray background.

2. THE DETECTOR

The H.E.S.S. experiment, located in the Khomas Highlands of Namibia ($23^\circ 16' 18''$ S, $16^\circ 30' 1''$ E, 1800 m above sea level), consists of a system of four IACTs (diameter 13 m, focal length 15 m, mirror area 107 m^2) in a square of 120 m side. The optics [1, 2] are of good quality resulting in a small (width $< 0.1^\circ$) point-spread-function (PSF) across the whole field of view (FOV). The H.E.S.S. cameras [3] are modular in design and contain all the necessary electronics for operation, triggering, and readout. Each camera contains 960 individual photomultiplier (PMT) pixels subtending 0.16° each, with Winston cone light concentrators, providing a 5° FOV with uniform response. An individual camera's trigger electronics divide the camera into overlapping 64 PMT sectors with a trigger requirement that a sector has a minimum number of pixels (3) with a signal above a threshold (5.3) in photoelectrons, coincident in an effective ~ 1.3 ns trigger window. A central trigger system [4] is used to require a multiple telescope coincidence (a minimum of two simultaneously triggered cameras) allowing for stereoscopic reconstruction of an EAS observed by the telescopes. More details on H.E.S.S. can be found in [5] (review), [6] (calibration), and [7] (analysis & performance).

The energy threshold of H.E.S.S. increases with zenith angle (Z) due to the increasing distance of the EAS maximum from the telescopes. This behavior is shown in Figure 1. The trigger threshold (no cuts) is 100 GeV near zenith, and the energy threshold remains below 1 TeV (after applying the standard γ -ray selection cuts) for zenith angles less than 60° , within which almost all H.E.S.S. observations are performed. The amount of observation time (live hours), at $Z=20^\circ$, required to detect ($>5\sigma$) a source for a range of fluxes is shown in Figure 1. For comparison to the previous generation of VHE instruments, HEGRA needed ~ 100 hours to detect 5σ from a 5% Crab Nebula

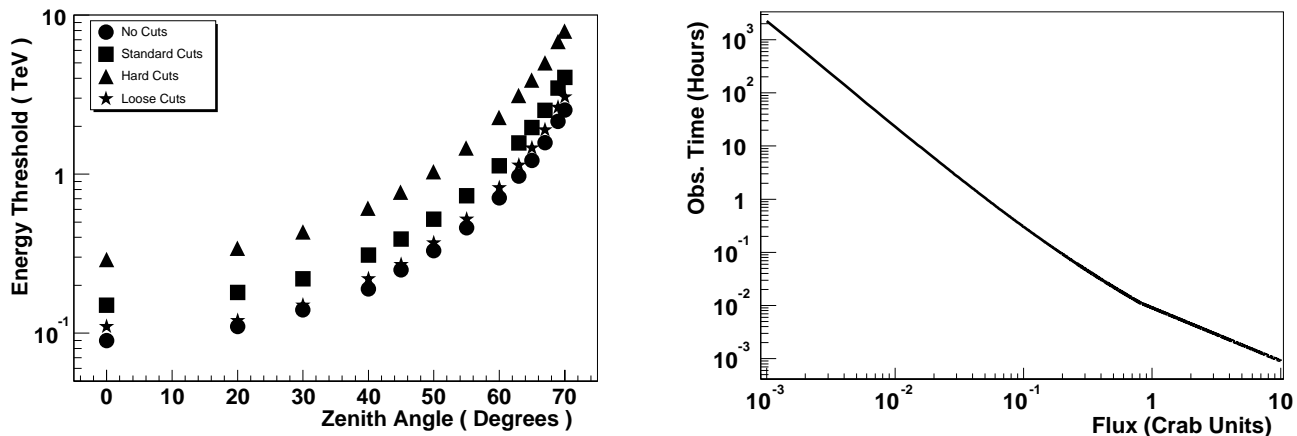


Figure 1: (Left) The energy threshold of H.E.S.S. before and after gamma-ray selection cuts *vs.* zenith angle. (Right) The observation time required to yield a 5σ detection at $Z=20^\circ$ *vs.* fraction of the Crab Nebula flux. The Crab Nebula is the brightest steady source in the VHE sky.

strength source, whereas H.E.S.S. only needs 1 hour of observations. H.E.S.S. has an average energy resolution of $\sim 15\%$ per event allowing for an accurate determination of a detected source's energy spectrum above the post-cuts energy threshold [7]. The systematic error on the photon index of a power-law fit to a measured spectrum is estimated to ~ 0.1 and the systematic error on the observed integral flux (or upper limit) is $\sim 20\%$.

3. RESULTS OVERVIEW

The unprecedented sensitivity of H.E.S.S. has allowed it to achieve many ground-breaking results. Among these is the detection of >30 sources of VHE γ -rays, from a variety of new and different source classes. Table I shows the sources published by H.E.S.S. Only ~ 10 sources of VHE γ -rays were known prior to the commencement of H.E.S.S. observations. In addition, all sources detected by H.E.S.S. are published with studies of their measured energy spectra and flux/spectral variability, allowing for detailed theoretical modeling of the non-thermal processes at work in the objects. Another achievement is the ability to perform, for the first time, high-resolution mapping of extended regions of the sky in VHE γ -rays (see e.g. [22]). This is enabled by the combination of the large FOV, the small angular resolution ($<0.1^\circ$), and low absolute pointing error ($<20''$ in each direction) of H.E.S.S., allowing for detailed studies of VHE source morphology, as well as making H.E.S.S. ideal for performing surveys for unknown VHE gamma-ray sources [20, 21].

As the number of sources discovered by H.E.S.S. is very large, individual discussion of their properties is beyond the scope of this contribution. Therefore, only a selection of important H.E.S.S. results are presented below.

3.1. GALACTIC PLANE SCAN

The Galactic Plane of the Milky Way, particularly the inner disk, contains a large population of objects capable of accelerating photons to VHE energies. These potential accelerators consist of the Galactic Center, supernova remnants (SNR), pulsar wind nebulae (PWN) and massive stars. Although 91 SNRs and 381 pulsars are known to exist [36, 37] in the central 60° in galactic longitude (l) and 6° in galactic latitude (b), only two objects (the Galactic Center [38] and the SNR RX J1713.7–3946 [39]) had been detected at VHE energies in this region prior to the commencement of H.E.S.S. observations. The unprecedented sensitivity of H.E.S.S. coupled with the high density of potential VHE sources motivated a deep (230 live-hours after data-quality selection) survey [20, 21] of this inner region in 2004. This survey, spanning $-30^\circ < l < 30^\circ$ and $-3^\circ < b < 3^\circ$, reached an average sensitivity of

Name	Association	Source Class	Size	Flux	Ref.
HESS J0534+220	Crab Nebula	PWN	Point-like	Steady	[8]
HESS J0835-456	Vela X	PWN	Extended	Steady	[9]
HESS J0852-463	RX J0852.0-4622 (Vela Jr)	SNR	Extended	Steady	[10, 11]
HESS J1103-234	1ES 1101-232	AGN (BL Lac)	Point-like	Steady	[12]
HESS J1104-382	Mkn 421	AGN (BL Lac)	Point-like	Variable	[13]
HESS J1230+123	M 87	AGN (FRI)	Point-like	Variable	[14]
HESS J1302-638	PSR B1259-63 / SS 2883	B/PWN	Point-like	Variable	[15]
HESS J1303-631	?	?	Extended	Steady	[16]
HESS J1418-609	G 313.3+0.1 (The Rabbit)	PWN	Extended	Steady	[17]
HESS J1420-607	K3 / PSR J1420-6048	PWN	Extended	Steady	[17]
HESS J1514-591	MSH 15 - 5 2 / PSR B1509-58	PWN	Extended	Steady	[18]
HESS J1555+111	PG 1553+113	AGN (BL Lac)	Point-like	Steady	[19]
HESS J1614-518	?	?	Extended	Steady	[20, 21]
HESS J1616-508	PSR J1617-5055	Scan (PWN)	Extended	Steady	[20, 21]
HESS J1632-478	IGR J16320-4751	Scan (XRB)	Extended	Steady	[21]
HESS J1634-472	IGR J16358-4726 / G 337.2+0.1	Scan (XRB/SNR)	Extended	Steady	[21]
HESS J1640-465	G 338.3-0.0 / 3EG J1639-4702	Scan (SNR/UID)	Extended	Steady	[20, 21]
HESS J1702-420	?	?	Extended	Steady	[21]
HESS J1708-410	?	?	Extended	Steady	[21]
HESS J1713-381	G 348.7+0.3	Scan (SNR)	Extended	Steady	[21]
HESS J1713-397	RX J1713.7-3946	SNR	Extended	Steady	[22-24]
HESS J1745-290	Sgr A* / Sgr A East?	Galactic Center	Point-like	Steady	[25, 26]
HESS J1745-303	3EG J1744-3011	Scan (UID)	Extended	Steady	[21]
HESS J1747-281	G 0.9+0.1	PWN	Point-like	Steady	[27]
HESS J1804-216	G 8.7-0.1 / PSR J1803-2137	Scan (PWN)	Extended	Steady	[20, 21]
HESS J1813-178	G 12.82-0.02	Scan (SNR)	Extended	Steady	[20, 21]
HESS J1825-137	PSR J1826-1334	PWN	Extended	Steady	[20, 21, 28, 29]
HESS J1826-148	LS 5039	B	Point-like	Variable	[30, 31]
HESS J1834-087	G 23.3-0.3 / W 41	Scan (SNR)	Extended	Steady	[20, 21]
HESS J1837-069	G 25.5+0.0 / AX J1838.0-0655	Scan (SNR)	Extended	Steady	[20, 21]
HESS J2009-488	PKS 2005-489	AGN (BL Lac)	Point-like	Steady	[32]
HESS J2158-302	PKS 2155-304	AGN (BL Lac)	Point-like	Variable	[33, 34]
HESS J2359-306	H 2356-309	AGN (BL Lac)	Point-like	Steady	[12, 35]

Table I: The H.E.S.S. source catalog: associations, source class, and references are shown, as well as whether the emission is point-like or extended, and whether the observed flux is steady or varies over time. For all the sources marked as 'Scan', the associations are based on positional coincidence(s) and therefore should only be considered as possible counterparts. The source class acronyms are Active Galactic Nucleus (AGN), Pulsar Wind Nebula (PWN), Supernova Remnant (SNR), Binary system (B) and unidentified (UID).

2% of the Crab Nebula flux above 200 GeV. In total, fourteen VHE γ -ray emitters were discovered in this survey (see Figure 2). All of these objects were found to be extended (i.e. not point-like) in size with respect to the PSF of H.E.S.S. Many of the fourteen new objects are identified, on the basis of positional coincidence, as corresponding to SNRs and PWN. However, for some of these objects no known counterpart exists at other wavelengths. The task of identifying these objects, and acceleration processes at work inside them, is the subject of future investigations. The differential energy spectra of all the objects are well-characterized by power-law functions ($dN/dE \sim E^{-\Gamma}$) with an average photon index ($\Gamma=2.3$). These hard spectra match that predicted from shock-wave acceleration in SNRs (see, e.g., [40, 41]) and as expected for the source spectrum of Galactic cosmic-rays (see, e.g., [42]). It should also be noted

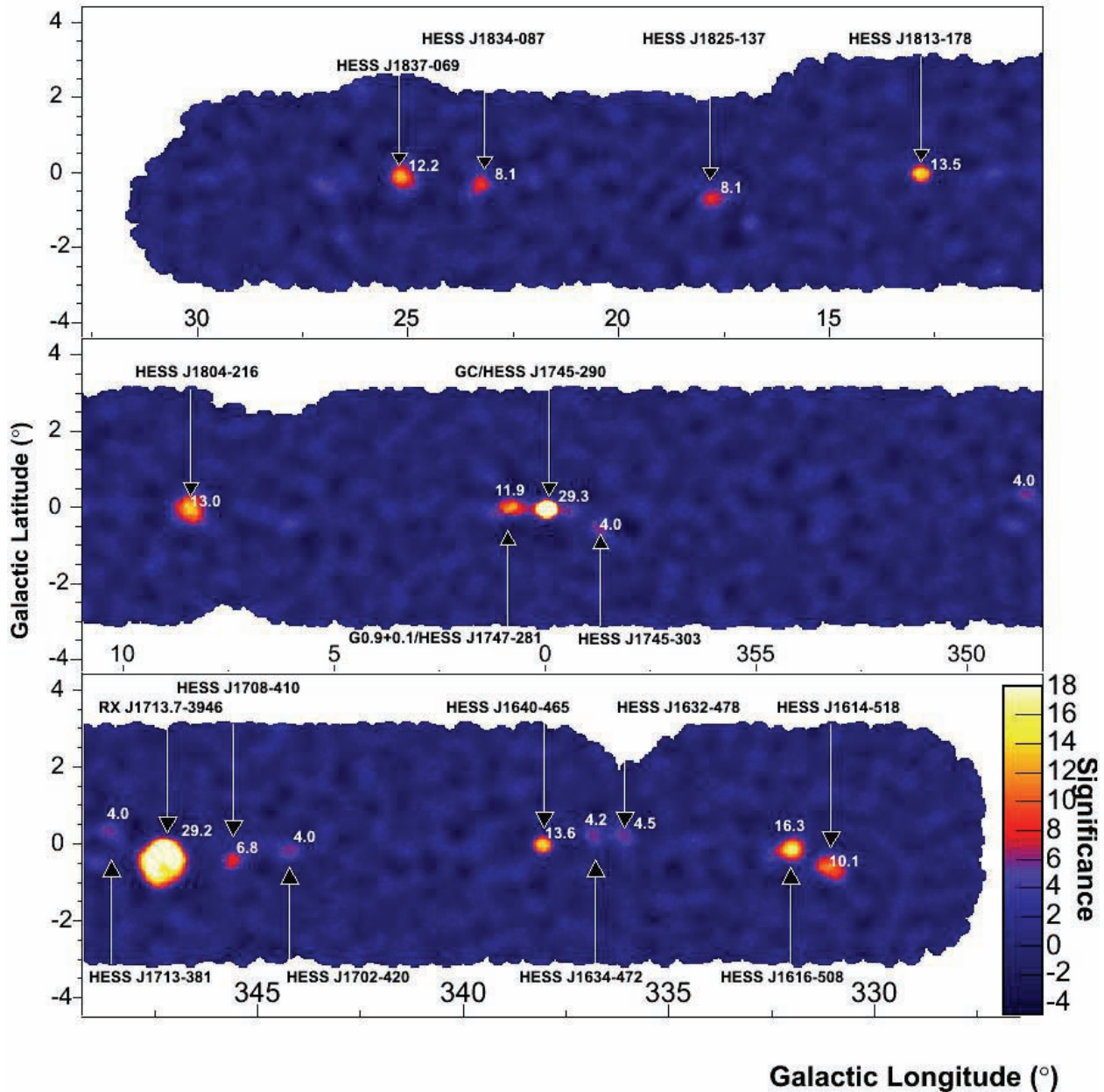


Figure 2: A sky map of the significance of the excess observed during the H.E.S.S. Galactic Plane survey in 2004. Fourteen new sources of VHE γ -rays are detected, as well as three sources (G 0.9+0.1 [27], the Galactic Center [25], & RX J1713.7–3946 [22]) previously seen by H.E.S.S. The numbers in the map give the statistical significance after accounting for all trials related to surveying a large number of sky positions. The significance scale is truncated at 18σ ; the signals from RX J1713.7–3946 and the Galactic Center exceed this level.

that two of these new VHE sources have been confirmed by the MAGIC collaboration to be VHE emitters [43, 44], and the properties (e.g size, flux, spectrum) measured by both experiments agree well.

3.2. THE GALACTIC CENTER

The Galactic Center region harbors a number of potential VHE emitters, and may be a site of VHE γ -ray production via annihilation of Dark Matter particles. A strong, steady VHE γ -ray source was detected [25, 26] at the Galactic

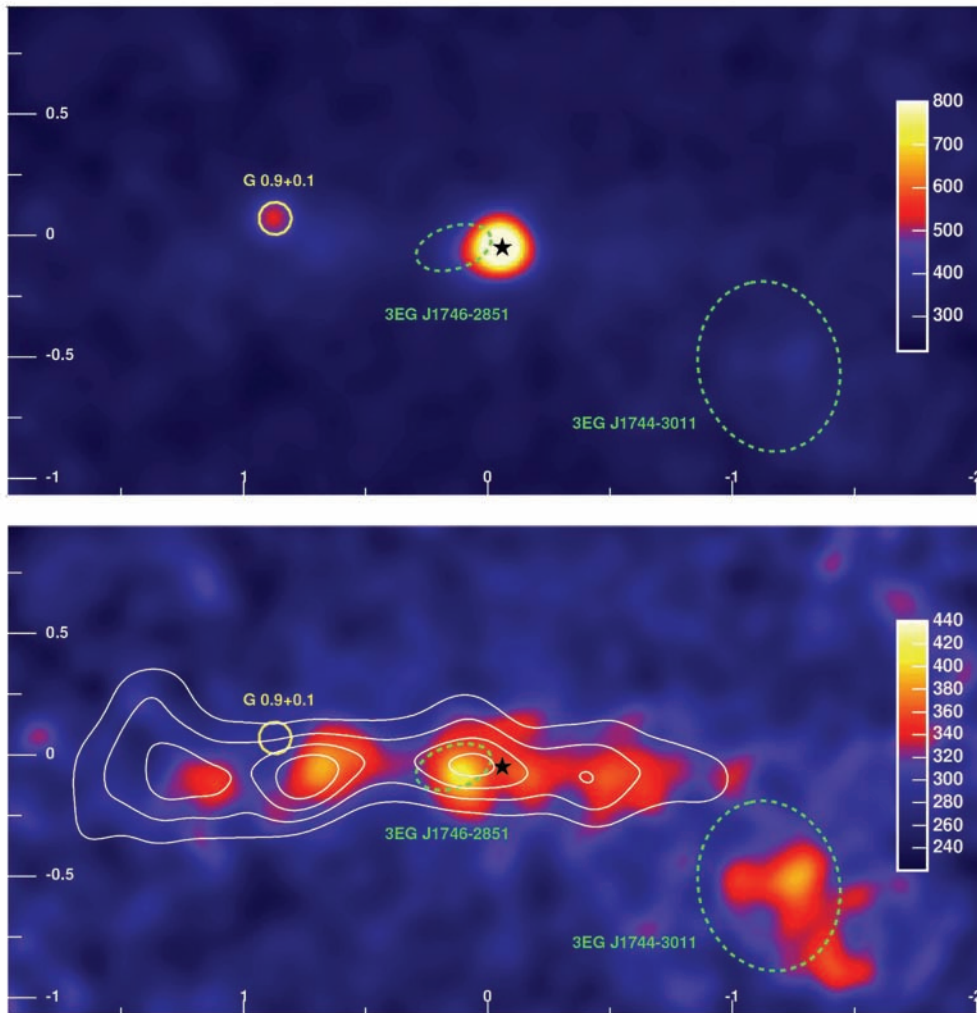


Figure 3: (Top) A γ -ray count map, smoothed with the point-spread-function of H.E.S.S., from the galactic center region. (Bottom) The same map after subtraction of the two dominant point sources. An extended band of γ -ray emission is seen. The white contour lines indicate the density of molecular gas as traced by its CS emission [46] and have been smoothed to match the PSF of H.E.S.S. The black star marks the position of Sgr A*, and the green ellipses mark the positions of two unidentified EGRET sources in the region.

Center during deep H.E.S.S. observations of this region (see Figure 3). The measured VHE spectrum is hard ($\Gamma \sim 2.3$) and follows a power-law behavior beyond 10 TeV, which is very difficult to produce via common Dark Matter annihilation channels. Although Dark Matter annihilation is very unlikely to be the dominant VHE γ -ray production mechanism [26], the astrophysical source of this VHE emission cannot be discerned from the location of the H.E.S.S. signal. Indeed, determination of the γ -ray counterpart may be impossible due to the density of potential emitters. Three astrophysical objects: the black hole Sgr A*, the SNR Sgr A East and the newly-discovered PWN G 359.95–0.04 are the most-likely counterparts. Interestingly, the X-ray flux of Sgr A* is known to vary dramatically from time to time. Detection of VHE-flux variability from the Galactic Center during one of these brief flares (or at any time since SNRs and PWN are not expected to be variable sources) would conclusively indicate that Sgr A* is the dominant VHE emitter. No variability of the VHE emission has been observed to date, however, H.E.S.S. has not observed the Galactic Center during any known X-ray flare either.

Galactic cosmic rays may interact with interstellar gas producing VHE γ -rays. Since the flux of VHE photons should be proportional to the amount of target material (e.g. interstellar gas), any VHE radiation should be higher

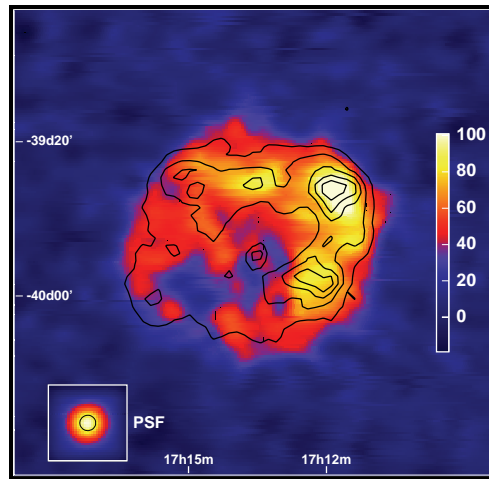


Figure 4: A sky map of γ -ray counts (excess events above background) from the SNR RX J1713.7–3946. The H.E.S.S. map is smoothed with the point-spread function of the instrument. A point-like source would appear as shown in the lower-left box marked PSF. The black contours correspond to those measured [48] by the ASCA X-ray satellite from 1 to 3 keV.

in regions of dense molecular clouds (such as the Galactic Center). Therefore the H.E.S.S. discovery [45] of a band of diffuse VHE γ -ray radiation tracing the Galactic Plane near the Galactic Center (see Figure 3) is very interesting. The VHE flux is essentially proportional to the gas-density in both its distribution in Galactic latitude and longitude. Interestingly, the VHE spectrum of the diffuse emission is much harder than would be produced if one assumes that the density of cosmic rays is the same at the Galactic Center as it is in the solar neighborhood. Since the VHE radiation is also proportional to the density of cosmic rays, this behavior indicates that the spectrum of cosmic rays is harder near the Galactic Center than elsewhere in the galaxy. A recently-active ($<10^4$ years ago) cosmic-ray accelerator, such as a pre-historic SNR near the Galactic Center, can plausibly explain this behavior.

3.3. SUPERNOVA REMNANTS

Supernovae are the fantastic explosions of massive stars. The remnants of these explosions are thought to be the principle sources of Galactic cosmic rays (up to $\sim 10^{15}$ eV). Acceleration of charged particles to energies greater than 100 TeV, through shock acceleration in these remnants, enables the production of VHE γ -rays via leptonic (inverse-Compton scattering of seed photons) and/or hadronic (nucleus-nucleus interaction) channels. The identification of SNRs as sources of VHE γ -rays by H.E.S.S. shows that these objects accelerate particles to at least 100 TeV. Interestingly, demonstration that the detected VHE γ -rays have a hadronic origin would “prove” that SNR are a source of hadronic cosmic-rays, solving the ~ 100 year old mystery of cosmic-ray origin.

3.3.1. SHELL-TYPE SNR

Shell-type SNR are those where the expansion of the explosion over time (i.e. shock wave) interacts with matter at the leading edge of the expansion, both sweeping up the new material as well as accelerating it to higher energies. This interaction produces a non-thermal shell-type structure that can be seen by instruments such as H.E.S.S. Two famous and very similar shell-type SNR, RX J1713.7–3946 and RX J0852.0–4622 (Vela Jr), have been detected [10, 22] by H.E.S.S. This shell-type structure can be seen in the γ -ray sky maps of both these objects (RX J1713.7–3946 is shown in Figure 4). The VHE morphology of the remnants matches that seen by X-ray satellites which detect photons produced by synchrotron radiation of relativistic electrons. While the morphology of the object is closely matched in the two energy ranges, suggesting a leptonic VHE γ -ray origin, there are subtle differences. For example, the H.E.S.S. measurements [23] of the spectrum of VHE photons over different regions of RX J1713.7–3946, show that the photon index does not change (see Figure 5), contrary to the behavior in X-rays [47]. Modeling the spectral

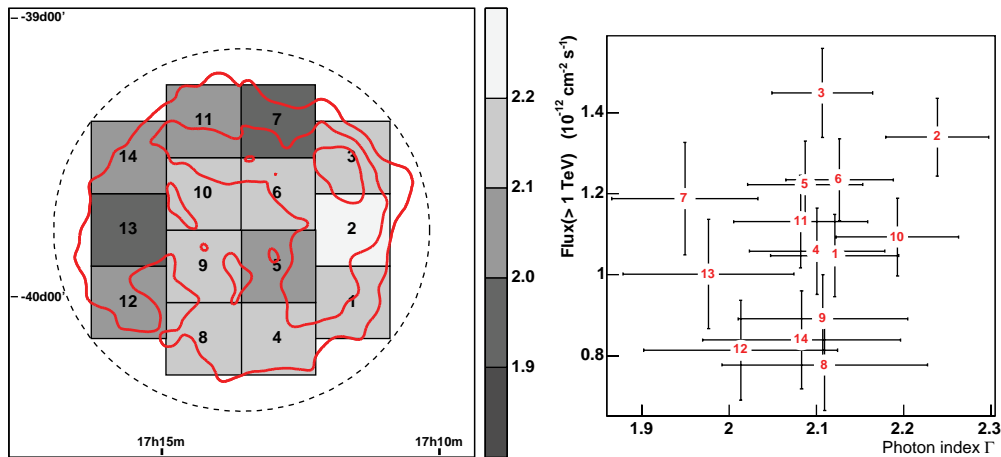


Figure 5: An illustration of the spatially-resolved spectral analysis for the SNR RX J1713.7–3946. (Left) The red contours represent H.E.S.S. excess contours and the 14 boxes represent the regions for which the spectrum was measured independently. The gray scale represents the measured photon index (Γ). (Right) The integral flux above 1 TeV *vs.* photon index measured for each of the 14 numbered boxes. A variation is seen in γ -ray flux, but not in photon index, across the remnant.

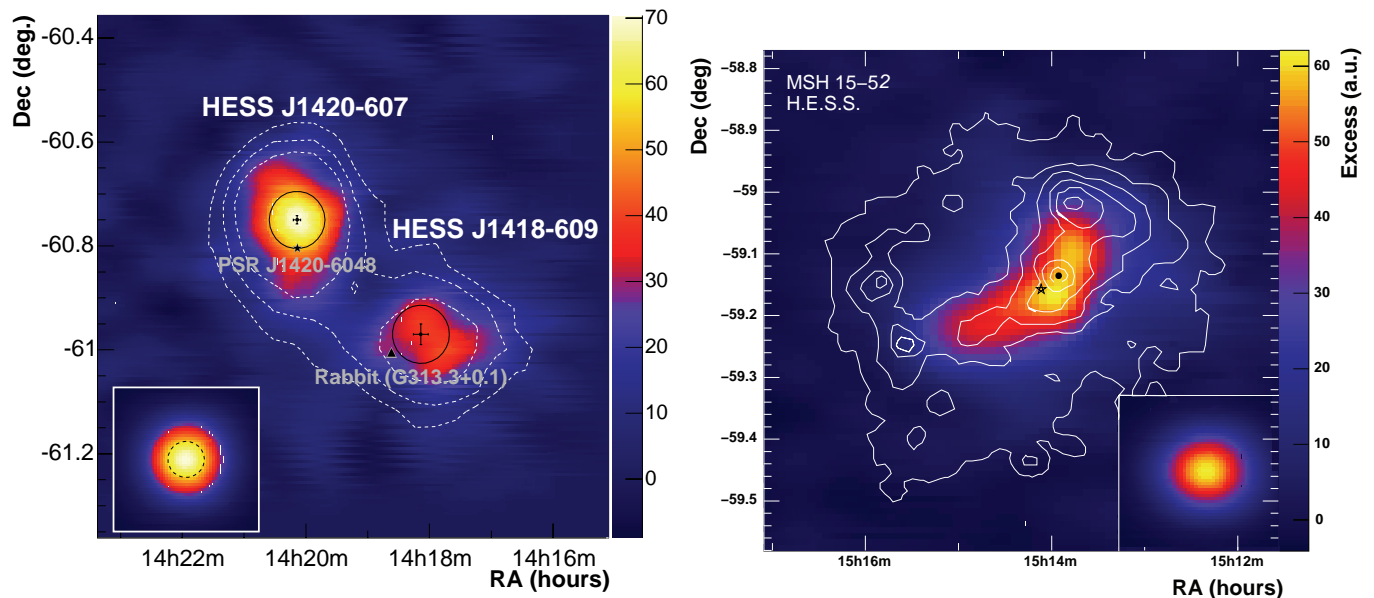


Figure 6: (Left) A smoothed excess sky map of the Kookaburra region. The contours represent H.E.S.S. significance. The black crosses and circles represent the fit positions and extensions, respectively of the H.E.S.S. excesses. The positions of PSR J1420-6048 and G 313+0.1 (the rabbit) are marked with a black star and triangle respectively. (Right) A smooth excess sky map from MSH 15–52. The white contour lines represent the X-ray count rate measured [50] by ROSAT. The black point and black star are located at the pulsar position and excess centroid, respectively. In both maps the bottom insets represent the appearance of a point-like excess.

energy distributions (SED) of these two shell-type SNRs (over 20 orders of magnitude in energy) strongly favors hadronic acceleration mechanisms [23]. However, definitive proof of a hadronic origin does not exist. Such proof likely requires measurements in the energy range of the GLAST and H.E.S.S. Phase-II experiments.

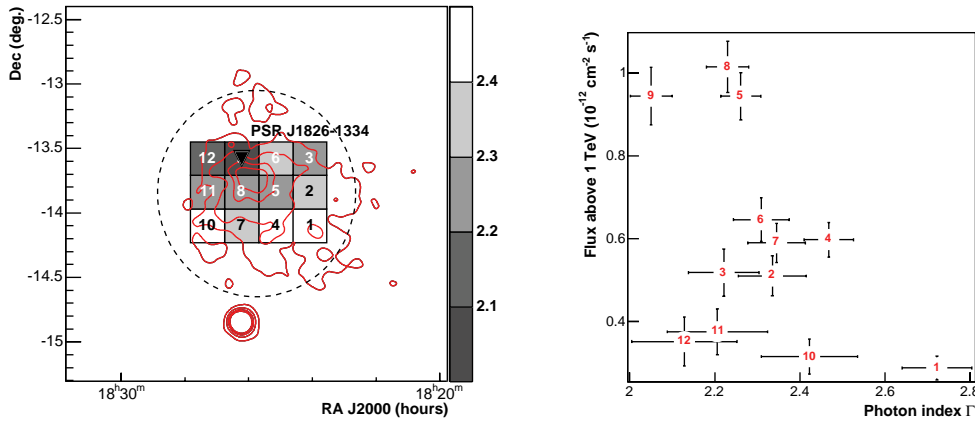


Figure 7: An illustration of the spatially-resolved spectral analysis for the PWN HESS J1825–137. (Left) The red contours represent H.E.S.S. excess contours and the 12 boxes represent the regions for which the spectrum was measured independently. The pulsar PSR J1826–1334 is shown by the black triangle. The gray scale represents the measured photon index (Γ). The circular structure towards the bottom is the microquasar LS 5039, a point-like emitter. (Right) The integral flux above 1 TeV *vs.* photon index measured for each of the 12 numbered boxes. A significant variation is seen in both γ -ray flux and photon index across the remnant. The photon index is softer (i.e. larger) as distance from the pulsar increases.

3.3.2. PULSAR WIND NEBULAE

Pulsar wind nebulae are SNRs where high-energy electrons accelerated in the vicinity of a pulsar emit synchrotron radiation (i.e. contain a synchrotron nebula). H.E.S.S. has detected at least ten PWN. Figure 6 shows three of these PWN. Surprisingly, the peak of the measured gamma-ray brightness is offset from the central pulsar position, and the morphology of the VHE γ -ray sky map is asymmetric. These two effects are found in most of the PWN detected by H.E.S.S. A plausible explanation [49] of this behavior is that it is due to the supernova expanding into a medium of inhomogeneous density. The shapes of the SEDs of the H.E.S.S. PWN are easily explained by models where the γ -ray emission is attributed to inverse-Compton scattering of ambient photons (primarily Cosmic Microwave Background photons) off a population of pulsar-powered synchrotron electrons in the nebula (see e.g. [18, 27]). Another interesting observation is that the VHE γ -ray spectrum of HESS J1825–137, corresponding to the PWN of PSR J1826-1334, is seen to soften (Γ increases) with distance to the pulsar [29]. This effect, shown in Figure 7, is the first time that energy-dependent morphology has been detected in the VHE γ -ray regime, and is best explained by the higher energy electrons (which produce the higher energy γ -rays) cooling faster than those at lower energies.

3.4. BINARY SYSTEMS

Although various incarnations of SNRs comprise the vast majority of the galactic H.E.S.S. sources, a different class of objects, binary systems, also are found to emit VHE γ -rays. These objects consist of a compact object (e.g a neutron star or pulsar) in orbit around a massive star (see Figure 8) for illustrations. The first such system discovered [15] to be a VHE γ -ray emitter, PSR B1259-63/SS 2883, consists of a millisecond pulsar in a highly eccentric orbit (~ 3.4 year period) around a Be-type star (a star surrounded by an equatorial disk). The VHE γ -ray emission was measured during a recent periastron passage in 2004 and was found to vary in VHE-photon flux, the first known case for a galactic VHE source, as the pulsar-position moved relative to the stellar disk, suggesting the interaction of the pulsar wind with the disk as the production-process for VHE γ -rays. The other object, LS 5039, a microquasar was initially detected [30] in the 2004 H.E.S.S. Galactic Plane survey. This object, is believed to be powered by accretion of matter from the massive star on to the compact object, creating jets (analogous to the much more massive quasar phenomena) within which VHE photons are generated. Although the H.E.S.S. discovery of microquasars as a class of VHE emitters is interesting, perhaps more so is the discovery [31] that the VHE flux

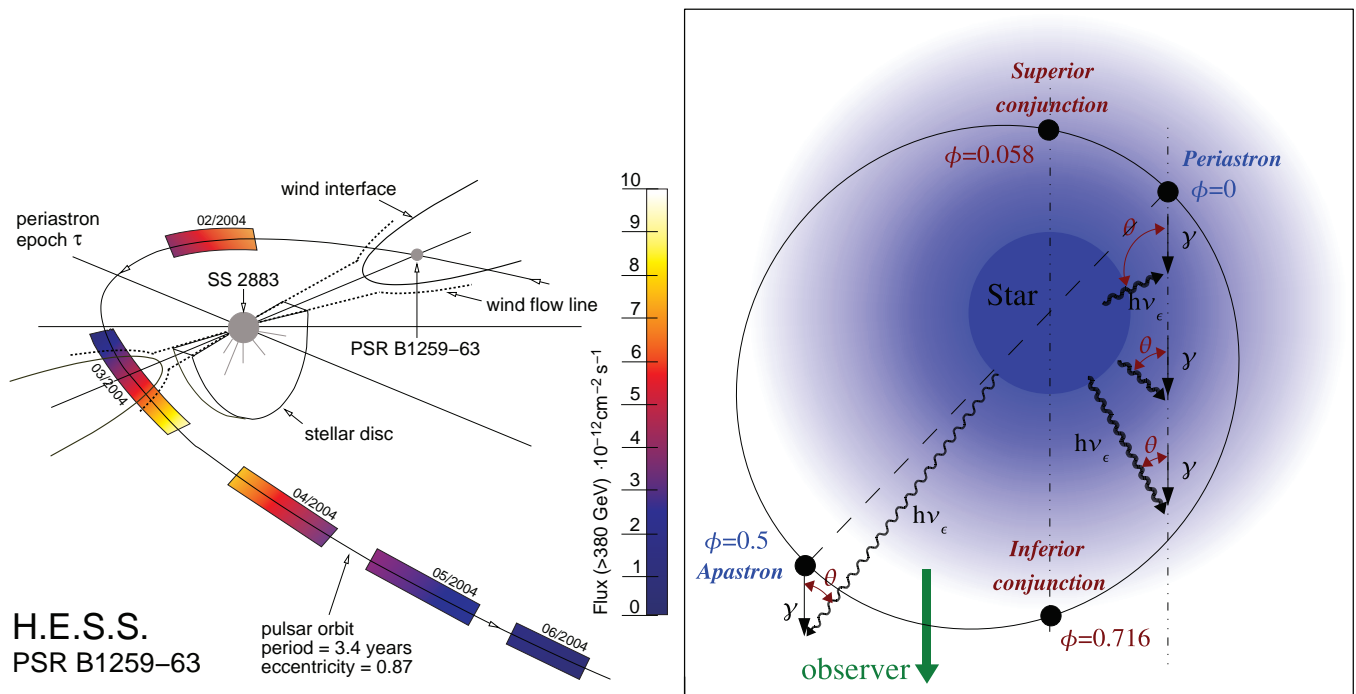


Figure 8: Illustrations of the two binary systems detected by H.E.S.S. (Left) The color-scale represents the variation of VHE γ -ray flux along the orbit of the pulsar PSR B1259–63. The location and size of the stellar disk are approximate. (Right) The microquasar LS 5039 as viewed from directly above. The orbit is inclined in the range $13^\circ < i < 64^\circ$ relative to the observer. The VHE γ -ray flux modulates precisely with the ~ 3.9 day orbital period of the system. The observed flux and spectrum are highest and hardest, respectively, near inferior conjunction, and lowest and softest, respectively, near superior conjunction. This is believed to be in part the effect of absorption of VHE γ -rays by the star's optical photons, possible when the γ -ray scattering angle, θ , exceeds zero.

modulates with the 3.9-day orbital period of the system. Both the photon index and VHE flux were found to vary with orbital phase (i.e. as the compact object moved around the star with respect to the observer's line of sight). This unique observation is the first clear indication of γ -ray absorption within an astrophysical source.

3.5. ACTIVE GALACTIC NUCLEI

Active Galactic Nuclei (AGN) represent the only class of extra-galactic objects known to emit VHE γ -rays. These objects are found in the core of at least 5% of all galaxies, and are characterized by very-bright (many orders of magnitude brighter than their host galaxy), highly-variable, non-thermal emission. They are believed to be powered by accretion of matter onto a super-massive (10^6 - 10^9 solar mass) black hole. In about 10% of all AGN (the radio-loud population), relativistic outflows of particles (known as relativistic jets) exist along the magnetic field of the black hole. Of particular interest to VHE astronomers are a class of radio-loud AGN known as blazars. Essentially all known VHE-bright AGN belong to this class. In blazars, one relativistic jet is pointed directly along the observer's line-of-sight (i.e. towards Earth).

H.E.S.S. has detected VHE emission from seven AGN, including four not previously known to be VHE-bright, and published strong (i.e. below the sensitivity of previous-generation instruments) upper limits on the VHE flux from nineteen other AGN. Of the seven VHE-bright AGN, all are blazars with the exception of M 87. Although relativistic jets are seen near the nucleus of M 87 (see Figure 9), it is not a blazar since the jets are inclined relative to the observer's line-of-sight.

VHE-flux variability is generally expected from blazars, since any intrinsic variability should be enhanced by the combination of relativistic Doppler effects in the jets and their orientation along the line-of-sight. Interestingly, the

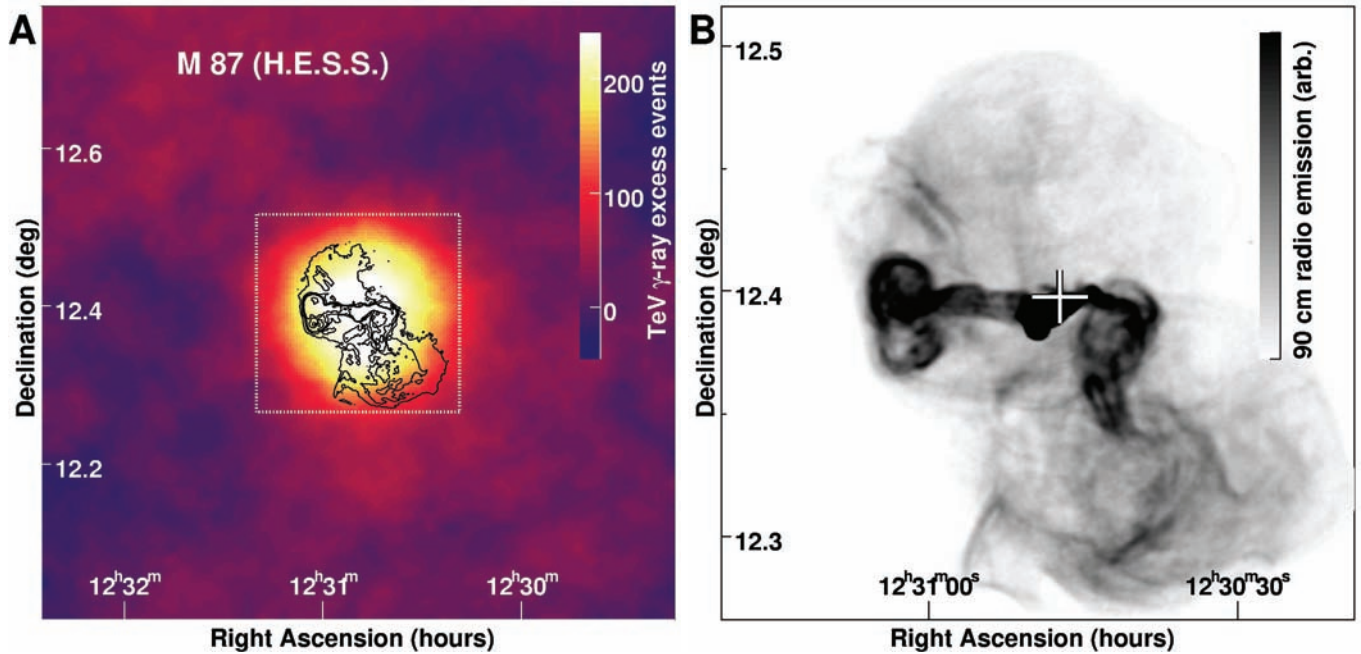


Figure 9: (Left) A γ -ray sky map of M87 as seen by H.E.S.S. The point-like signal appears extended due to the PSF of the instrument. The black contours reflect the structure of M87 at radio wavelengths. (Right) The appearance of M87 at radio wavelengths. The white cross represents the location (near the nucleus) of the H.E.S.S. excess. The radio data, adapted from [51], clearly show the jet structure.

VHE emission seen from four of the H.E.S.S. blazars is constant in time. The non-blazar M87 is again exceptional as its VHE flux is variable on the time-scale of days [14]. This surprising discovery implies that the emission from M87 originates from a small region very near the Schwarzschild radius of its black hole, and not in more distant regions of the kpc-scale jet. It also should be noted that many H.E.S.S. AGN observations are performed simultaneously with instruments at other wavelengths (e.g. X-ray, optical, & radio). Since blazars are known to be highly variable, simultaneity is required for accurate modeling (see, e.g., [34, 35]) of their broad-band SED.

The spectra of the H.E.S.S. AGN are generally soft ($\Gamma > 3$) compared to the H.E.S.S. galactic sources ($\Gamma \sim 2.3$). Since VHE photons are attenuated by pair-production on the Extragalactic Background Light (EBL) a softening, increasing with distance, of the observed VHE spectrum is expected for distant objects. The VHE emission from two relatively distant H.E.S.S. blazars, 1ES 1101–232 ($z=0.186$) and H 2356–309 ($z=0.165$), has surprisingly hard spectra. This observation allowed the determination [12] of upper limits on the poorly-measured EBL density which are much lower than the density previously believed, and within a factor of two of the minimum level established by integrating all light from known galaxies. The new upper limits imply that the universe is much more transparent to VHE photons than previously believed, and that the VHE horizon, beyond which all photons are attenuated, is more distant. Ultimately, this increases the possibilities for new extragalactic source detections.

4. CONCLUSION

With VHE observations being performed by H.E.S.S., as well as by other third-generation VHE atmospheric Cherenkov instruments such as CANGAROO-III, MAGIC and VERITAS, it is clear that the future of VHE γ -ray astronomy is bright. Should VHE astronomy progress similarly to X-ray astronomy or lower-energy γ -ray astronomy, the number of sources is expected to increase dramatically as shown in Figure 10. With this increased source catalog, a greater understanding of the non-thermal sky will be achieved, since new conclusions will be based on modeling of large populations of source-types, instead a handful of "unique" objects.

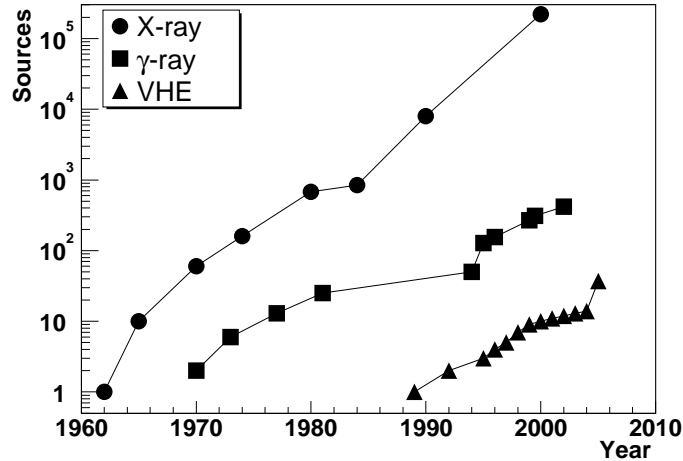


Figure 10: The "Kifune plot": Shown are the number of detected sources in X-rays, lower-energy γ -rays, and VHE γ -rays versus time.

Although the H.E.S.S. collaboration is continuing to make interesting observations, an upgrade of the current detector is underway. This upgrade [52], H.E.S.S. Phase-II, involves the addition of the largest-ever (30m diameter) Cherenkov telescope to the center of the existing array. This new telescope will have a six-times larger mirror area and two-times finer camera pixelization than the existing telescopes, enabling both more light collection and better-resolved EAS images. Ultimately, this addition will increase the sensitivity of the current experiment by a factor of two and lower the energy threshold to ~ 30 GeV, providing a good overlap in energy with the upcoming GLAST satellite.

Acknowledgments

The support of the Namibian authorities and of the University of Namibia in facilitating the construction and operation of H.E.S.S. is gratefully acknowledged, as is the support by the German Ministry for Education and Research (BMBF), the Max Planck Society, the French Ministry for Research, the CNRS-IN2P3 and the Astroparticle Interdisciplinary Programme of the CNRS, the U.K. Particle Physics and Astronomy Research Council (PPARC), the IPNP of the Charles University, the South African Department of Science and Technology and National Research Foundation, and by the University of Namibia. We appreciate the excellent work of the technical support staff in Berlin, Durham, Hamburg, Heidelberg, Palaiseau, Paris, Saclay, and in Namibia in the construction and operation of the equipment.

References

- [1] Bernlöhner, K., et al., *Astroparticle Physics*, **20**, 111, 2003
- [2] Cornils, R., et al., *Astroparticle Physics*, **20**, 129, 2003
- [3] Vincent, P., et al., *Proc. of the 28th ICRC (Tsukuba)*, 2887, 2003
- [4] Funk, S., et al., *Astroparticle Physics*, **22**, 285, 2004
- [5] Hinton, J., *New Astronomy Reviews*, **48**, 331, 2004
- [6] Aharonian, F., et al. (H.E.S.S. Collaboration), *Astroparticle Physics*, **22**, 109, 2004
- [7] Benbow, W., *Proc. of Towards a Network of Atmospheric Cherenkov Detectors VII (Palaiseau)*, 163, 2005
- [8] Aharonian, F., et al. (H.E.S.S. Collaboration), *A&A*, **457**, 899, 2006

- [9] Aharonian, F., et al. (H.E.S.S. Collaboration), *A&A*, **448**, L43, 2006
- [10] Aharonian, F., et al. (H.E.S.S. Collaboration), *A&A*, **437**, L7, 2005
- [11] Aharonian, F., et al. (H.E.S.S. Collaboration), *ApJ*, **in press**, 2006
- [12] Aharonian, F., et al. (H.E.S.S. Collaboration), *Nature*, **440**, 1018, 2006
- [13] Aharonian, F., et al. (H.E.S.S. Collaboration), *A&A*, **437**, 95, 2005
- [14] Aharonian, F., et al. (H.E.S.S. Collaboration), *Science*, **in Press**, 2006
- [15] Aharonian, F., et al. (H.E.S.S. Collaboration), *A&A*, **442**, 1, 2005
- [16] Aharonian, F., et al. (H.E.S.S. Collaboration), *A&A*, **439**, 1013, 2005
- [17] Aharonian, F., et al. (H.E.S.S. Collaboration), *A&A*, **456**, 245, 2006
- [18] Aharonian, F., et al. (H.E.S.S. Collaboration), *A&A*, **435**, L17, 2005
- [19] Aharonian, F., et al. (H.E.S.S. Collaboration), *A&A*, **448**, L19, 2006
- [20] Aharonian, F., et al. (H.E.S.S. Collaboration), *Science*, **307**, 1938, 2005
- [21] Aharonian, F., et al. (H.E.S.S. Collaboration), *ApJ*, **636**, 777, 2006
- [22] Aharonian, F., et al. (H.E.S.S. Collaboration), *Nature*, **432**, 75, 2004
- [23] Aharonian, F., et al. (H.E.S.S. Collaboration), *A&A*, **449**, 223, 2006
- [24] Aharonian, F., et al. (H.E.S.S. Collaboration), *A&A*, **in press**, 2006
- [25] Aharonian, F., et al. (H.E.S.S. Collaboration), *A&A*, **425**, L13, 2004
- [26] Aharonian, F., et al. (H.E.S.S. Collaboration), *Phys Rev Let*, **in press**, 2006 [astro-ph/0610509]
- [27] Aharonian, F., et al. (H.E.S.S. Collaboration), *A&A*, **432**, L25, 2005
- [28] Aharonian, F., et al. (H.E.S.S. Collaboration), *A&A*, **445**, L25, 2005
- [29] Aharonian, F., et al. (H.E.S.S. Collaboration), *A&A*, **in press**, 2006 [astro-ph/0607548]
- [30] Aharonian, F., et al. (H.E.S.S. Collaboration), *Science*, **309**, 746, 2005
- [31] Aharonian, F., et al. (H.E.S.S. Collaboration), *A&A*, **in press**, 2006 [astro-ph/0607192]
- [32] Aharonian, F., et al. (H.E.S.S. Collaboration), *A&A*, **436**, L17, 2005
- [33] Aharonian, F., et al. (H.E.S.S. Collaboration), *A&A*, **430**, 865, 2005
- [34] Aharonian, F., et al. (H.E.S.S. Collaboration), *A&A*, **442**, 177, 2005
- [35] Aharonian, F., et al. (H.E.S.S. Collaboration), *A&A*, **455**, 461, 2006
- [36] Green, D.A., *Bull Astron Soc India*, **32**, 335, 2004
- [37] Manchester, R.N., et al., *AJ*, **129**, 1993, 2005
- [38] Kosack, K., et al., *ApJ*, **608**, L97, 2004
- [39] Enomoto, R., et al., *Nature*, **416**, 823, 2002
- [40] Berezhko, E.G. & Völk, H.J., *Astroparticle Physics*, **7**, 183, 1997
- [41] Berezhko, E.G. & Völk, H.J., *A&A*, **357**, 283, 2000
- [42] Jones, F.C., et al., *ApJ*, **547**, 264, 2001
- [43] Albert, J., et al., *ApJ*, **637**, L41, 2006
- [44] Albert, J., et al., *ApJ*, **643**, L53, 2006
- [45] Aharonian, F., et al. (H.E.S.S. Collaboration), *Nature*, **439**, 695, 2006
- [46] Tsuboi, M., et al., *ApJS*, **120**, 1, 1999
- [47] Cassam-Chenaï, G., et al., *A&A*, **427**, 199, 2004
- [48] Uchiyama, Y., et al., *Publ Astron Soc Japan*, **54**, L73, 2002
- [49] Blondin, et al., *ApJ*, **563**, 806, 2001
- [50] Trussoni, E., et al., *A&A*, **306**, 581, 1996
- [51] Owen, F.N., et al., *ApJ*, **543**, 611, 2000
- [52] Punch, M., 2005, *Proc. of Towards a Network of Atmospheric Cherenkov Detectors VII (Palaiseau)*, 379, 2005